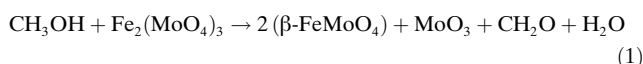


# Redox Behavior of Fe-Mo-O Catalysts Studied by Ultrarapid In Situ Diffraction\*\*

S. D. M. Jacques, O. Leynaud, D. Strusevich,  
A. M. Beale, G. Sankar, C. M. Martin, and P. Barnes\*

The term “Fe-Mo-O” is used to denote a mixed-phase catalyst system as used, for example, in the production of formaldehyde, which is an important building block for complex chemicals in many consumer products. Almost all formaldehyde is manufactured by either: 1) dehydrogenation of a methanol-rich air mixture over a silver catalyst or 2) direct oxidation of methanol over a Fe-Mo-O-based catalyst.<sup>[1,2a]</sup> The latter process is advantageous in that the exothermic reaction can be carried out at comparatively lower temperatures, typically 375–350 °C, and the catalyst offers comparatively higher activity and selectivity.<sup>[2b]</sup> The mechanism is assumed to follow a Mars/van Krevelen like process of oxidative dehydrogenation of hydrocarbons and has been demonstrated for an industrial Fe-Cr-Mo-O preparation.<sup>[3]</sup> Methanol oxidation proceeds with a partial reduction of the active iron molybdate  $\text{Fe}_2(\text{MoO}_4)_3$  phase [Eq. (1)], followed by catalyst regeneration:<sup>[4,5]</sup>



There have been several notable studies on Fe-Mo-O catalysts<sup>[3,6–14]</sup> that covered aspects of catalytic activity,

deactivation, and mechanism. In particular, the Mo/Fe ratio is considered to be important; industrial preparations use a Mo/Fe ratio greater than 1.5:1 comprising a mixture of two phases  $\text{Fe}_2(\text{MoO}_4)_3$  and  $\text{MoO}_3$ . It is thought that the primary function of  $\text{MoO}_3$  is to provide a reservoir of molybdenum to balance losses through sublimation at reactor hot spots that would otherwise prevent regeneration of the active phase and lead to the formation of  $\text{Fe}_2\text{O}_3$ , which favors total oxidation.<sup>[1,7,15]</sup> However, there have not been any previous diffraction studies that focus on the interplay between these phases and their effect on the catalytic reaction and regeneration. Herein, we show the importance of observing these reactions by using rapid time-resolved in situ powder diffraction; in particular, we capture the responses of the Fe-Mo-O catalyst under accelerated aging conditions and show the importance of the multiple-phase form in maintaining catalyst longevity.

A special environmental cell system has been designed to apply redox cycling conditions to catalyst material while collecting (in situ) powder diffraction data on the synchrotron; this cell is illustrated in Figure 1 and described with operational details in the Experimental Section.

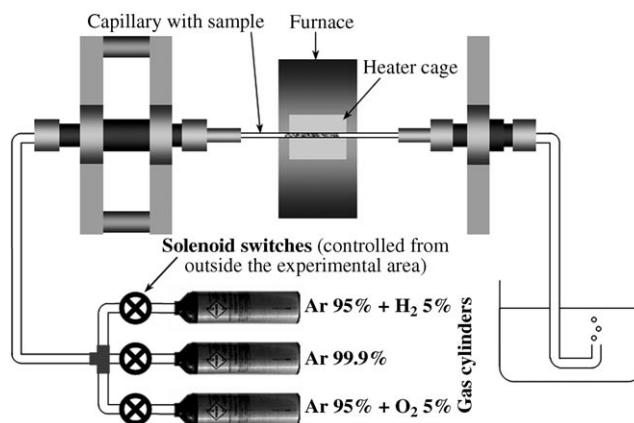


**Figure 1.** Schematic representation of the redox environmental cell consisting of a capillary furnace and gas-delivery system. The incident and diffracted synchrotron X-ray beams are in a perpendicular plane (to the diagram), with the exit window of the furnace spanning an angular range of 120°.

Diffraction patterns of the catalyst material, both as prepared and after reduction, were analyzed first to confirm the starting materials and basic methodology. The three-component phases expected,  $\text{Fe}_2(\text{MoO}_4)_3$ ,  $\text{MoO}_3$ , and  $\beta\text{-FeMoO}_4$ , account for all the constituent peaks in the diffraction patterns once allowance has been made for differential thermal expansion up to the operating temperature of 472 °C: For  $\text{Fe}_2(\text{MoO}_4)_3$ , its two very similar allotropes<sup>[19]</sup> can be accommodated by using the high-temperature form<sup>[20]</sup> extrapolated to 472 °C; for  $\text{MoO}_3$ , in-house high-temperature neutron data<sup>[21]</sup> were necessary to unravel the mixed (positive/negative) expansion contributions; for  $\beta\text{-FeMoO}_4$ , reliable data<sup>[22]</sup> could be found only for ambient conditions, and so the diffraction peaks at 472 °C were identified by indexing the remaining peaks (with the Crysfire

[\*] Dr. S. D. M. Jacques, Dr. O. Leynaud, D. Strusevich, Prof. P. Barnes  
Industrial Materials Group  
Materials Chemistry Centre, Department of Chemistry  
University College London  
20 Gordon Street, London WC1H 0AJ (UK)  
and  
Department of Crystallography  
Birkbeck College  
Malet Street, London WC1E 7HX (UK)  
Fax: (+44) 207-631-6803  
E-mail: barnes@img.cryst.bbk.ac.uk

Dr. A. M. Beale  
Department of Inorganic Chemistry and Catalysis  
Sorbonnelaan 16, 3584 CA, Utrecht (The Netherlands)  
Prof. G. Sankar  
The Royal Institution  
21 Albemarle Street, London W1X 4BS (UK)  
Dr. C. M. Martin  
CLRC Daresbury Laboratory  
Daresbury, Warrington WA4 4AD (UK)

[\*\*] The authors acknowledge the EPSRC for financial support, the staff of Daresbury Laboratory, and the engineers Paul Stukas (Birkbeck College) and Mike Sheehy (Royal Institution) for design/construction of the furnace.

Supporting information for this article is available on the WWW under <http://www.angewandte.org> or from the author.

program<sup>[23]</sup>) by using the ambient unit cell as a starting guide. The peak positions of the three phases at 472 °C were then all refined independently against the experimental patterns using the Celref program.<sup>[24]</sup> This approach provided an essential starting set of parameters (Table 1) for the subse-

**Table 1:** Space groups, starting unit-cell parameters, and weight fractions for the three-component phases.<sup>[a]</sup>

Phase	Space group	Unit-cell parameters [Å]	Initial fraction [%]	Reduced fraction [%]
Fe <sub>2</sub> (MoO <sub>4</sub> ) <sub>3</sub>	<i>Pbcn</i>	<i>a</i> = 12.88; <i>b</i> = 9.206; <i>c</i> = 9.323	51	27
β-FeMoO <sub>4</sub>	<i>C12/m1</i>	<i>a</i> = 10.36; <i>b</i> = 9.447; <i>c</i> = 7.107 β = 106.4°	< 1	19
MoO <sub>3</sub>	<i>Pnma</i>	<i>a</i> = 14.20; <i>b</i> = 3.702; <i>c</i> = 3.989	49	54

[a] These data were obtained by fitting simulated patterns to the diffraction patterns for the initial catalyst and the same after reduction at 472 °C.

quent multiphase Rietveld refinements of the in situ patterns obtained during the redox cycles; no peaks remained unexplained, though there was a residual intensity mismatch for some MoO<sub>3</sub> peaks during the Rietveld refinement because of the preferred orientation of MoO<sub>3</sub>, which is typical of lamellar structures<sup>[21]</sup> (an example fit is given in the Supporting Information).

Figure 2a shows the time-resolved in situ patterns obtained during a reduction-oxidation-reduction cycle at 472 °C. The collection time for each pattern was 30 seconds and the sequence covers 60 minutes spanning almost a complete cycle.

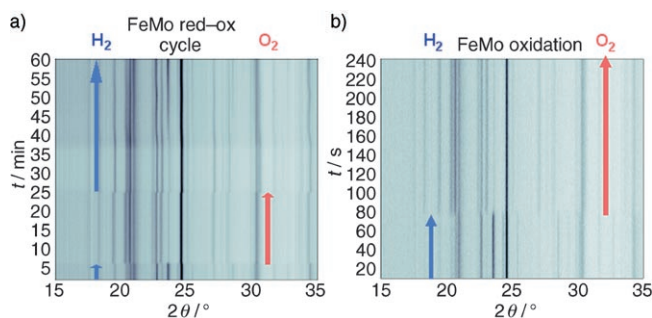


**Figure 2.** Contour images of in situ powder diffraction from a Fe-Mo-O catalyst at 472 °C under successive reducing (red) and oxidizing (blue) atmospheres: a) 120 × 30 s patterns that show the end of one reduction cycle, a full oxidation cycle, and part of a second reduction step; b) an ultra-rapid acquisition (patterns every 2 s), thus illustrating the extreme rapidity of the oxidation stage.

The change in diffraction patterns on introduction of the oxidizing gas (at 5 minutes) is dramatic, thus appearing to be discontinuous on the minute timescale. By comparison, the changes during subsequent reduction (25–60 min) are far more gradual. The sequence of changes in the position of peaks is somewhat complicated by a small movement of the

sample capillary in the diffractometer as the gas is changed: thus, there are peak shifts at 5 minutes that arise from both structural changes and capillary movement, whereas the immediate shifts at 25 minutes are entirely because of capillary movement. This effect was effectively “subtracted out” in the subsequent data analysis. Multiphase Rietveld structure refinement (cyclic mode of Fullprof<sup>[25]</sup> using WinPLOT software<sup>[26]</sup>) was performed over 120 patterns (Figure 3a), in which the unit cells and scale factors (effec-

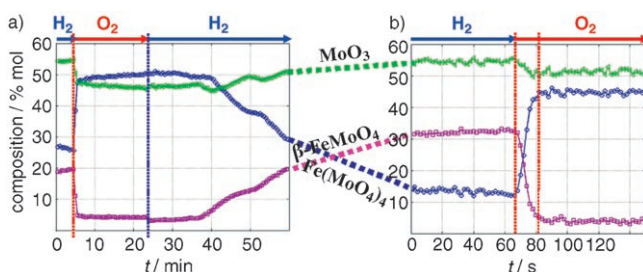
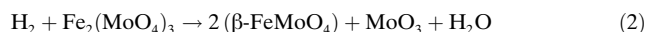


**Figure 3.** Phase composition (% mol weight fractions) of Fe<sub>2</sub>(MoO<sub>4</sub>)<sub>3</sub>, β-FeMoO<sub>4</sub>, and MoO<sub>3</sub> obtained by multiphase Rietveld fitting to the data shown in Figure 2 (same gas environment notation): a) Variations on the minute timescale that show incomplete reduction, even after 36 min; b) capturing the rapid oxidation stage on a second timescale.

tively molecular-weight fractions) were allowed to vary but the fractional atomic coordinates and the profile parameters were kept fixed because of the unavoidable preferred orientation effects mentioned previously. The resulting variations in weight fraction versus time are given in Figure 3a; the general trends are clear over and above the irregularities (e.g., ≈ 50 min), which arise from inhomogeneities in gas flow/penetration through the large specimen agglomerates required to pack the capillary (see the Experimental Section). The Supporting Information shows that these irregularities can be smoothed out by using larger specimen capillaries (4 mm in diameter), but at the expense of data speed/resolution, which is required for the oxidation stage (see later).

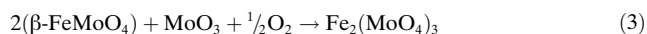
The disproportionate rapidity of the oxidation stage, relative to reduction, required reexamination while pushing the system performance to its limit. The result is shown in Figure 2b, which shows the oxidation stage captured in two-second diffraction intervals. Multiphase Rietveld refinements were performed on the two-second diffraction patterns that span the transition to quantify this further. The resulting scatter is unavoidably increased, nevertheless the time profile obtained (Figure 3b) clearly shows the progression of this transition and that the oxidation reactions are virtually completed within 15 seconds. At present, one can only speculate on why there should be such a huge difference in the reduction and oxidation rates: First, one notes that the standard redox potential of +0.77 V for Fe<sup>3+</sup> + e<sup>−</sup> → Fe<sup>2+</sup> rather suggests a favored reduction (forward direction) though one should also consider the observation<sup>[14]</sup> that this process might occur through two steps at the catalyst surface, first Mo<sup>6+</sup> to Mo<sup>5+</sup> before Fe<sup>3+</sup> to Fe<sup>2+</sup>. Other explanations that relate to higher anionic mobilities for the β-FeMoO<sub>4</sub>

phase, which aid the solid-state transport of oxygen during oxidation, remain questionable in light of the rapid oxidation rates observed. A more intriguing possibility, for which there is some supporting evidence,<sup>[27,28]</sup> concerns the physicochemical nature of the reduction reaction itself [see Eq. (2)],

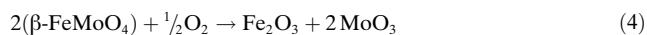


whereby  $\text{H}_2\text{O}$  production will block access of hydrogen to the Fe-Mo-O active sites during reduction; by contrast, known rapid oxygen uptake<sup>[29]</sup> clearly aids the reoxidation process. Importantly, one also notes that the presence of other crystalline Mo/Fe reduced phases are clearly ruled out by the diffraction data.

In conclusion, this study has demonstrated the power of ultra-rapid in situ powder diffraction for obtaining new insight into the high-temperature solid-state redox processes that occur in a mixed catalyst system. The combination of intense synchrotron wiggler radiation, X-ray optics, and an ultra-rapid/high-resolution detector enables one to follow both slow reactions and those that are too fast for capture by conventional laboratory or synchrotron techniques. It is possible to rationalize the behavior according to a Mars/van Krevlen type process: the  $\text{Fe}_2(\text{MoO}_4)_3$  phase undergoes reduction in an atmosphere of 5%  $\text{H}_2/\text{Ar}$  according to equation (2) and subsequent regeneration in an atmosphere of 5%  $\text{O}_2/\text{Ar}$  according to Equation (3):



The speed of the redox processes at 472 °C has been uniquely determined: Even though these are multiphase solid-state reactions, the oxidation stage is found to be extremely fast; oxidation is effectively completed within 15 seconds at 472 °C, in contrast to the reduction stage, which is incomplete even after 36 minutes. This difference in rate appears to be contrary to the existing viewpoint (e.g., Pernicone<sup>[12]</sup>) that reduction of  $\text{Fe}_2(\text{MoO}_4)_3$  is easier than oxidation of  $\beta\text{-FeMoO}_4$ . This difference in reactivity will be critical for maintaining phase stability and catalyst activity. The absence of any additional phases suggests that reaction (3) proceeds so quickly that other solid-state side reactions that lead to deactivation [e.g., Eq. (4)] are avoided:



Therefore, we have demonstrated that the addition of an excess of  $\text{MoO}_3$  in the as-prepared catalyst is beneficial for maintaining the stability of the active phase as well as replenishing any sublimed molybdenum that might occur. Finally, we note that although there have been previous attempts to capture redox processes that occur in single-phase systems this investigation is the first diffraction study, as far as the authors are aware, of such rapid reactions within a mixed-phase solid-state system. Many other catalytic systems can now realistically become candidates for detailed study by this method, including the optimization of catalyst composition and working temperature.

## Experimental Section

The industrial-like iron molybdate catalyst was prepared with a Mo/Fe atomic ratio of 3:1 by using a coprecipitation method similar to that by Soares et al.<sup>[6]</sup> using appropriate amounts of  $[\text{Mo}_7(\text{NH}_4)_6\text{O}_{24}]\cdot 4\text{H}_2\text{O}$  and  $[\text{Fe}(\text{NO}_3)_3]\cdot 9\text{H}_2\text{O}$ . The product was calcined at 375 °C for 2 h and then pelletized, crushed, and coarsely sieved to obtain suitable agglomerates for mounting inside the furnace quartz capillary.

The environmental cell system consists primarily of a capillary furnace and gas-delivery system (Figure 1). The furnace is sufficiently small (100 × 47 mm) to facilitate connection of the capillary to a gas inlet/outlet. A thermocouple adjacent to the sample regulates the temperature, the recorded temperatures corrected by means of prior calibrations with a probable error of  $\pm 10^\circ\text{C}$ , which is confirmed by the subsequent regression analysis of the high-temperature  $\text{MoO}_3$  unit-cell dimensions. Inert (100% Ar), reducing (5%  $\text{H}_2/\text{Ar}$ ), and oxidizing (5%  $\text{O}_2/\text{Ar}$ ) gases can be passed through the heated sample capillary during data collection, with remote start/stop control. The sample, contained in the 1-mm diameter quartz capillary, is protected from loss into the flowing gas by quartz wool plugs.

All data collection was carried out on station 6.2 of the SRS synchrotron (Daresbury, UK). This station has been recently commissioned<sup>[16,17]</sup> as a high-flux multipole wiggler beamline facility for materials processing. In powder diffraction mode, the optics system delivers an incident X-ray footprint of  $0.5 \times 3$  mm for capillary operation, with a selected incident wavelength of 1.400 Å. Diffraction data were collected by using the RAPID2 detector,<sup>[16]</sup> which realizes a medium-high angular resolution (0.06°) at ultra-high count rates (20 MHz global) through its multi-wire/multi-electronic-channel mode of operation, over a nominal  $2\theta$  range of 60°. The resulting rapid powder diffraction patterns are of sufficient quality for Rietveld<sup>[18]</sup> structure refinement.

Received: August 15, 2005

Published online: December 2, 2005

**Keywords:** iron · oxidation · redox chemistry · synchrotron · X-ray diffraction

- [1] B. Stiles, T. A. Koch, *Catalyst Manufacturer*, 2nd ed., Marcel Dekker, New York, **1995**, p. 197.
- [2] a) R. Crichton, *Informally Speaking, The Formaldehyde Newsletter from Perstorp Formox*, Claes Lundström, Perstorp Formox AB, SE-284 80 Perstorp, Sweden (or <http://www.perstorpformox.com>), **2003**, Spring/Summer, pp. 12–13; b) A. Andersson, *Informally Speaking, The Formaldehyde Newsletter from Perstorp Formox*, Claes Lundström, Perstorp Formox AB, SE-284 80 Perstorp, Sweden (or <http://www.perstorpformox.com>), **2003**, Autumn/Winter, pp. 10–12.
- [3] D. S. Lafyatis, G. Creten, G. F. Froment, *Appl. Catal. A* **1994**, *120*, 85–103.
- [4] A. V. Demidov, I. G. Danilova, G. N. Kustova, L. M. Plyasova, N. G. Skomorokhova, L. L. Sedova, V. B. Nakrokhin, B. I. Popov, *Kinet. Catal.* **1992**, *33*, 910–914.
- [5] G. Alessandrini, L. Cairati, P. Forzatti, P. L. Villa, F. Trifirò, *J. Less-Common Met.* **1977**, *54*, 373–386.
- [6] A. P. V. Soares, M. Farinha Portela, A. Kiennemann, L. Hilaire, J. M. M. Millet, *Appl. Catal. A* **2001**, *206*, 221–229.
- [7] A. P. V. Soares, M. Farinha Portela, A. Kiennemann, *Catal. Commun.* **2001**, *2*, 159–164.
- [8] A. P. V. Soares, M. Farinha Portela, A. Kiennemann, L. Hilaire, *Chem. Eng. Sci.* **2003**, *58*, 1315–1322.
- [9] J.-L. Li, Y.-X. Zhang, C.-W. Liu, Q.-M. Zhu, *Catal. Today* **1999**, *51*, 195–199.

- [10] J. H. Wilson III, C. G. Hill, Jr., J. A. Dumesic, *J. Molec. Catal.* **1990**, 61, 333–352.
- [11] C. J. Machiels, W. H. Cheng, U. Chowdhry, W. E. Farneth, F. Hong, E. M. McCarron, A. W. Sleight, *Appl. Catal.* **1986**, 25, 249–256.
- [12] N. Pernicone, *Catal. Today* **1991**, 11, 85–91.
- [13] V. Diakov, D. Lafarga, A. Varma, *Catal. Today* **2001**, 67, 159–167.
- [14] H. Zhang, J. Shen, X. Ge, *J. Solid State Chem.* **1995**, 117, 127–135.
- [15] M. Bowker, R. Holroyd, A. Elliott, P. Morrall, A. Alouche, C. Entwistle, A. Toerncrona, *Catal. Lett.* **2002**, 83, 165–176.
- [16] A. Berry, W. I. Helsby, B. T. Parker, C. J. Hall, P. A. Buksh, A. Hill, N. Clague, M. Hillon, G. Corbett, P. Clifford, A. Tidbury, R. A. Lewis, R. J. Cernik, P. Barnes, G. E. Derbyshire, *Nucl. Instrum. Methods Phys. Res. Sect. A* **2003**, 513, 260–263.
- [17] R. J. Cernik, P. Barnes, G. Bushnell-Wye, A. J. Dent, G. P. Diakun, J. V. Flaherty, G. N. Greaves, E. L. Heeley, W. Helsby, S. D. M. Jacques, J. Kay, T. Rayment, A. Ryan, C. C. Tang, N. J. Terrill, *J. Synchrotron Radiat.* **2004**, 11, 163–170.
- [18] H. M. Rietveld, *J. Appl. Crystallogr.* **1969**, 2, 65–71.
- [19] A. W. Sleight, L. H. Brixner, *J. Solid State Chem.* **1973**, 7, 172–174.
- [20] W. T. A. Harrison, *Mater. Res. Bull.* **1995**, 30, 1325–1331.
- [21] E. Lalik, PhD thesis, University of London (UK) **2003**.
- [22] A. W. Sleight, B. L. Chamberland, J. F. Weiher, *Inorg. Chem.* **1968**, 7, 1093–1098.
- [23] R. Shirley, *The CRYSFIRE System for Automatic Powder Indexing: User's Manual*, The Lattice Press, Surrey, **1999**.
- [24] J. Laugier, B. Bochu, Celref software, part of the LMGP Suite using the GETSPEC software referred to by: U. D. Altermatt, I. D. Brown, *Acta Crystallogr. Sect. A* **1987**, 43, 125–130.
- [25] J. Rodríguez-Carvajal, FULLPROF: A Program for Rietveld Refinement and Pattern Matching Analysis, *Abstr. Satellite Meeting Powder Diffraction, XV Congr. It. Union Cryst.*, **1990**, 127.
- [26] “WinPLOT: a Windows tool for powder diffraction patterns analysis”: T. Roisnel, J. Rodríguez-Carvajal, *Mater. Sci. Forum* **2001**, 378, 118–123.
- [27] N. Pernicone, F. Lazzerin, G. Lanzvecchia, *J. Catal.* **1968**, 10, 83–84.
- [28] A. P. V. Soares, M. F. Portela, A. Klennemann, *Catal. Rev.* **2004**, 47, 125–174.
- [29] K. Otsuka, Y. Wang, *Appl. Catal.* **2001**, 222, 145–161.

---